Acta Pharmacologica Sinica

www.nature.com/aps

ARTICLE

Targeting PI3Kα overcomes resistance to KRas^{G12C} inhibitors mediated by activation of EGFR and/or IGF1R

Wei-liang Qi[1,2,3], Hui-yu Li[1,2], Yi Wang[1], Lan Xu[1], Jie-ting Deng[4], Xi Zhang[1], Yu-xiang Wang[1] and Ling-hua Meng[1,2,4]

Although several KRas^{G12C} inhibitors have displayed promising efficacy in clinical settings, acquired resistance developed rapidly and circumvented the activity of KRas^{G12C} inhibitors. To explore the mechanism rendering acquired resistance to KRas^{G12C} inhibitors, we established a series of *KRAS*^{G12C}-mutant cells with acquired resistance to AMG510. We found that differential activation of receptor tyrosine kinases (RTKs) especially EGFR or IGF1R rendered resistance to AMG510 in different cellular contexts by maintaining the activation of MAPK and PI3K signaling. Simultaneous inhibition of EGFR and IGF1R restored sensitivity to AMG510 in resistant cells. PI3K integrates signals from multiple RTKs and the level of phosphorylated AKT was revealed to negatively correlate with the anti-proliferative activity of AMG510 in *KRAS*^{G12C}-mutant cells. Concurrently treatment of a novel PI3Kα inhibitor CYH33 with AMG510 exhibited a synergistic effect against parental and resistant *KRAS*^{G12C}-mutant cells in vitro and in vivo, which was accompanied with concomitant inhibition of AKT and MAPK signaling. Taken together, these findings revealed the potential mechanism rendering acquired resistance to KRas^{G12C} inhibitors and provided a mechanistic rationale to combine PI3Kα inhibitors with KRas^{G12C} inhibitors for therapy of *KRAS*^{G12C}-mutant cancers in future clinical trials.

Keywords: AMG510; KRas^{G12C}; PI3K; drug resistance; combination therapy

Acta Pharmacologica Sinica (2023) 44:1083–1094; https://doi.org/10.1038/s41401-022-01015-0

INTRODUCTION

KRAS is a critical driver of oncogenesis and one of the most frequently mutated oncogenes in cancer, with mutations in approximately every seven cancer patients [1]. Mutations in *KRAS* account for about 85% of mutants in *RAS* family members, while mutations at codon 12 predominate in *KRAS* [2]. Physiologically, KRas cycles between an active GTP-bound state and an inactive GDP-bound state [3], which is regulated by guanine nucleotide exchange factors (GEFs) that facilitate the release of GDP, and GTPase activating/accelerating proteins (GAPs) that strengthen the relatively poor intrinsic GTPase activity of KRas. The GTP-bound KRas is able to activate the downstream signaling such as phosphoinositide 3-kinase (PI3K) [4] and mitogen-activated protein kinase (MAPK) [5] pathways and thus regulate cell survival, proliferation and migration. Mutations at codon 12 of *KRAS* dramatically weaken its association with GAPs [4], resulting in persistent GTP-bound active state and eventually the development of cancer [6–8].

Although *KRAS* is one of the first discovered oncogenes and has long been considered as a promising therapeutic target, the high affinity between KRas and GTP limited the development of directly targeted inhibitors [9]. Recently, the unique characteristics of one of the *KRAS* mutants, *KRAS*^{G12C}, have been exploited for the design of covalent inhibitors that specifically bind to the mutated cysteine residue [10–14]. These compounds irreversibly bind to the Cys12 residue and lock the KRas protein in the inactive KRas-GDP state [15], which displayed potent activity against cancers harboring *KRAS*^{G12C} mutation in preclinical and clinical studies [16]. AMG510 (Sotorasib) is the first KRas^{G12C} inhibitor approved by the Food and Drug Administration (FDA) for treatment of *KRAS*^{G12C}-mutated locally advanced or metastatic non-small cell lung cancer (NSCLC) [17, 18].

Though AMG510 and other KRAS^{G12C} covalent inhibitors such as MRTX849 have shown promising efficacy, the objective response rate was 36% for AMG510 [19] or 53.3% for MRTX849 [12, 20] in NSCLC patients harboring *KRAS*^{G12C} mutation, which is much lower than those obtained with osimertinib for the therapy of epidermal growth factor receptor (EGFR)-mutated NSCLC patients (80%) [21] or with alectinib for the therapy of anaplastic lymphoma kinase (ALK)-positive NSCLC patients (82.9%) [22]. Adaptive resistance may circumvent the efficacy of KRas^{G12C} inhibitors. Treatment of *KRAS*^{G12C}-mutated cancer cells with KRas^{G12C} inhibitors for 24–48 h resulted in adaptive feedback activation of receptor tyrosine kinases (RTKs) [23, 24], rebound of the MAPK/PI3K pathway [10, 25] or upregulation of Aurora kinase [26], which might compromise the efficacy of KRas^{G12C} inhibitors. However, these observations might not reflect the mechanisms of acquired resistance developed after a long-term treatment of KRAS^{G12C} inhibitors. By sequencing tumor samples from a total of 38 patients who had developed acquired resistance to MRTX849, a recent study found that diverse genomic and histologic alterations might mediate resistance to KRas^{G12C} inhibitors, including secondary mutation at codon 13, 61, 68, 95, 96 in *KRAS* and amplification of the *KRAS*^{G12C} allele [27]. Meanwhile, systematic

[1]Division of Anti-tumor Pharmacology, Shanghai Institute of Materia Medica, Chinese Academy of Sciences, No.501 Haike Road, Shanghai 201203, China; [2]University of Chinese Academy of Sciences, No. 19A Yuquan Road, Beijing 100049, China; [3]College of Pharmacy, Nanchang University, No. 461, Bayi Road, Nanchang 330006, China and [4]School of Chinese Materia Medica, Nanjing University of Chinese Medicine, Nanjing 210023, China
Correspondence: Yu-xiang Wang (yxwang@simm.ac.cn) or Ling-hua Meng (lhmeng@simm.ac.cn)

Received: 4 July 2022 Accepted: 18 October 2022
Published online: 21 November 2022

studies are still needed to identify mechanisms conferring acquired resistance to $KRas^{G12C}$ inhibitors and develop combination therapy that may delay or overcome the acquired resistance.

In this study, we established a series of cell lines with acquired resistance to AMG510 by exposing the parental cells to increasing concentrations of AMG510. We found that activation of RTKs in resistant cells attenuated the activity of AMG510 in $KRAS^{G12C}$-mutant cells, while different cells might depend on different RTKs to develop the acquired resistance. The PI3K pathway integrates signaling downstream of various RTKs, and we found that the sensitivity to AMG510 is inversely related to the level of phosphorylated AKT in $KRAS^{G12C}$-mutant cells. Combinatorial inhibition of $KRas^{G12C}$ and PI3Kα achieved significant inhibition on the growth of xenografts derived from AMG510-resistant $KRAS^{G12C}$-mutant cells. These data revealed the potential mechanism rendering acquired resistance to $KRas^{G12C}$ inhibitors and provided a mechanistic rationale to test $KRas^{G12C}$ inhibitors in combination with PI3Kα inhibitors in future clinical trials.

MATERIALS AND METHODS

Compounds and reagents

CYH33 was provided by Shanghai HaiHe Biopharma Co. Ltd (Shanghai, China). AMG510, Erlotinib, and Linsitinib were purchased from Selleck Chemicals (Houston, TX, USA). For in vitro experiments, all compounds were dissolved in dimethyl sulfoxide (DMSO, Sigma, St. Louis, MO, USA) at the concentrations of 10 mM and stored at −20 °C. For in vivo studies, CYH33 and AMG510 were dissolved in normal saline containing 0.5% Tween 80 (v/v; Sangon Biotech, Shanghai, China) and 1% CMC-Na (m/v; SINOPHARM, Beijing, China). The human EGF (R&D System, RN 62253–63–8, Minneapolis, MN, USA) was dissolved in 10 mM acetic acid at the concentration of 200 μg/mL and stored at −80 °C. The human IGF1 (R&D System, 291-G1-200, Minneapolis, MN, USA) was dissolved in PBS at the concentration of 200 μg/mL and stored at −80 °C.

Cell lines and cell culture

The $KRAS^{G12C}$-mutant cells H2122, H358, H23, SW1463, SW837, MIA PaCa-2, H1792, and Calu-1 were purchased from ATCC, and H2291, HCC44, H2030, SW756 cells were purchased from COBIOER (Nanjing, China). KYSE410 cells were kindly provided by Dr. Hideaki Shimada (Department of Surgery, Toho University School of Medicine). All cell lines were authenticated by analyzing short-tandem repeats (STR) by Genesky Biotechnologies Inc. (Shanghai, China). H2122, H23, H2291, HCC44, H2030, H358, and KYSE410 cells were maintained in RPMI-1640 medium, Calu-1 cells were maintained in McCoy's 5A medium, and SW1463, SW837, and SW756 cells were maintained in Leibovitz's L-15 medium. All the media were supplemented with 10% fetal bovine serum. MIA PaCa-2 cells were maintained in DMEM supplemented with 10% fetal bovine serum and 2.5% horse serum. AMG510-resistant cells were established by exposing H358, H23, Calu-1, MIA PaCa-2, and SW837 cells to increasing concentrations of AMG510 as described previously [28]. H2122, H23, H2291, HCC44, H2030, H358, Calu-1, and KYSE410 cells were incubated in humidified atmosphere containing 5% CO_2 at 37 °C. SW1463, SW837, and SW756 cells were maintained in humidified atmosphere at 37 °C.

Cell proliferation assay and colony formation assay

Cell proliferation was evaluated using the sulforhodamine B (SRB, Sigma, St. Louis, USA) assay as described previously [29]. The inhibitory rate was calculated by using the formula: $(OD_{DMSO} - OD_{compound})/(OD_{DMSO} - OD_{d0}) \times 100\%$. To assess colony formation ability, cells seeded in 6-well plates were treated with indicated compounds for 10 days. Colonies were fixed with precooled methanol and stained with 0.1% crystal violet. Images were recorded with the ChemiDoc™ Touch Imaging System (Bio-Rad, Hercules, CA, USA), and quantified by Image J (https://imagej.nih.gov/ij/). As SW837 R cells migrated during colony formation, no clear spots of cell colonies were formed. We quantified the colonies by dissolving crystal violet and measuring *OD* values at 590 nm.

Western blotting

Cell lysates were prepared and standard Western blotting was performed with antibodies against AKT (#4691), phospho-AKT (Ser473) (#4060), ERK (#4695), phospho-ERK (Thr202/Tyr204) (#4370), phospho-RB (Ser807/811) (#8516), RB (#9313), phospho-IGF1R (Tyr1135/1136) (#2969), IGF1R (#1453), phospho-EGFR (Tyr1068) (#3777), EGFR (#4267), phospho-AXL (Tyr702) (#5724), AXL (#8661), phospho-IRS1 (Ser636/639) (#2388), phospho-GAB1 (Tyr627) (#3233), GAB1 (#3232) (Cell Signaling Technology, Danvers, MA, USA), SOS2 (#AB85831), GRB2 (#AB49876) (Abcam, Cambridge, UK), EGF (#A13615), IGF1 (#A11985) (Abclonal, Wuhan, China), GAPDH (#60004-1-1G) (Proteintech, Chicago, IL, USA), β-Actin (A5441) (Sigma, St. Louis, MO, USA). Images were captured with the ChemiDoc™ Touch Imaging System (Bio-Rad, Hercules, CA, USA). The intensity of protein bands was quantified by Image J.

Flow cytometry

Samples for analysis of cell cycle distribution were prepared as previously described [30]. Data were collected with an ACEA NovoCyte™ (Agilent Biosciences, Santa Clara, CA, USA) and analyzed with NovoExpress™ software (Agilent Biosciences, Santa Clara, CA, USA).

Combination analysis

Cells were treated with single agent alone or in combination, and cell proliferation was determined by SRB assay. The combination indexes (CI) in Calu-1, HCC44, Calu-1 R, H23 R, SW837 R, and MIA PaCa-2 R cells was analyzed by CalcuSyn software (Biosoft, Cambridge, UK). The combinatorial effect in Calu-1 C and H2122 cells was determined by the Bliss independence model with the formula: $y_{Bliss} = y_1 + y_2 - y_1{}^*y_2$, where y_1 *and* y_2 represent the inhibitory rates of each single agent [31]. The CI was determined with the formula: y_{Bliss}/y_{1+2}, where y_{1+2} represents the inhibitory rate of the combination. A CI = 1 indicated an additive effect, a CI > 1 indicated antagonism, and a CI < 1 indicated synergism.

Sanger sequencing

Total RNA was extracted using RNA easy Mini Kit (QIAGEN, Valencia, CA, USA) following manufacture's instruction. RNA was reverse transcribed into cDNA using HiScriptIIRT SuperMix for PCR. PCR was performed to generate target gene and the PCR products were sequenced by Sangon Biotech (Shanghai, China) with the primers as follows: KRAS-F (5′-TCCCAGGTGCGGGAGAG-3′) and KRAS-R (5′-AGTCATGGTCACTCTCCCCA-3′).

Quantitative RT-qPCR

Total RNA from cells was extracted using RNA easy Mini Kit (QIAGEN, Valencia, CA, USA) following manufacture's instruction. RNA was reverse transcribed into cDNA using HiScriptIIRT SuperMix for qPCR (+gDNA wiper) (Vazyme, R223-01, Nanjing, China) and then used for real-time quantitative PCR using SYBR Green Supermix (Bio-Rad). Primers employed were as follows: EGF-F (5′-TGTCCACGCAATGTGTCTGAA-3′), EGF-R (5′-CATTATCGGGTGAGGAACAACC-3′), IGF1-F (5′-GCTCTTCAGTTCGTGTGTGGA-3′), and IGF1-R (5′-GCCTCCTTAGATCACAGCTCC-3′).

Phospho-RTK array

The level of phosphorylated RTKs was measured using Human Phospho-RTK array kit (R&D Systems, ARY001B, Minneapolis, MN, USA). Cells were washed with cold PBS and lysed using the provided lysis buffer supplemented with phosphatase and

protease inhibitors. Membranes were incubated with cellular lysates containing 300 μg of protein overnight. On the next day, membranes were washed with provided washing buffer and exposed with chemiluminescent reagent. The blots were quantified by Image J.

Animal studies

All experiments were carried out according to the Institutional Ethical Guidelines on Animal Care and were approved by the Institute of Animal Care and Use Committee at Shanghai Institute of Materia Medica. Female BALB/c athymic nude mice aged 4–5-weeks were obtained from the Shanghai Institute of Materia Medica (Shanghai, China). Xenografts derived from Calu-1 or Calu-1 C cells were established by injecting cells suspended in Matrigel subcutaneously into the right side of axillary. Tumor sections were cut into pieces of about 40 mm^3 and then transplanted subcutaneously into mice. When the tumor volume achieved an average size of 100 mm^3, animals were randomized to receive vehicle control, AMG510 (30 mg/kg), CYH33 (20 mg/kg), or combined AMG510 and CYH33 for 21 days. The treatment in mice with AMG510 mono-therapy or the combination was suspended on day 22 and the mice were off the administration for 14 days. Body weight was recorded by electronic balance and the tumor volume was measured using micro calipers twice per week. The tumor volume (V) was calculated using the formula $V = a^2*b/2$, a and b represented the tumor's width and length, respectively. The relative tumor volume (RTV) and the treatment-to-control ratio (T/C) were calculated.

Statistical analysis

Data were analyzed by GraphPad Prism 8.0 (GraphPad, La Jolla, CA, USA) and shown as mean ± standard deviation (SD) from at least three independent experiments unless otherwise indicated. Statistical significance was determined by unpaired t test (with Welch's correction) between two groups, or one-way ANOVA for three or more groups.

RESULTS

AMG510 displayed variable anti-proliferative activity in $KRAS^{G12C}$-mutant cells

To investigate potential mechanisms underlying the efficacy of $KRas^{G12C}$ inhibitors, we evaluated the anti-proliferative activity of AMG510 against a panel of 12 $KRAS^{G12C}$-mutant cell lines originated from different tissue types, and classified the cell lines into three groups according to their sensitivity to AMG510. As shown in Fig. 1a, H358, Calu-1, MIA PaCa-2, SW837 and H23 cells were defined as AMG510-seneitive cells, in which AMG510 at 1 μM inhibited the cell growth by more than 50%. H2122 cells were considered as AMG510-resistant cells with inhibitory rate less than 20%. The rest of the cell lines exhibited moderate sensitivity to AMG510 with inhibitory rate between 20% and 50%. PI3K and MAPK pathways are regulated by Ras and play indispensable roles in cell growth and survival [32–34]. Notably, the level of phosphorylated ERK had been considered as a potential biomarker to monitor the efficacy of $KRas^{G12C}$ inhibitors [10]. Thus, we dissected PI3K and MAPK signaling pathways in representative sensitive H358 and Calu-1 cells, moderate-sensitive HCC44 cells and resistant H2122 cells treated with AMG510 for 2 h. As shown in Fig. 1b, AMG510 inhibited the phosphorylation of both ERK and AKT in H358 and Calu-1 cells, while it blocked the phosphorylation of ERK but not AKT in HCC44 cells. Neither phospho-ERK nor phospho-AKT was affected in H2122 cells. As it has been known that $KRas^{G12C}$ inhibitors attenuated cell proliferation by arresting cells at G1 phase [26], we then detected the effect of AMG510 on cell cycle distribution. H358 and Calu-1 cells were significantly arrested at G1 phase after the treatment of AMG510 for 24 h, while the cell cycle distribution was not affected in HCC44 and H2122 cells (Fig. 1c). As a gatekeeper of G1/S phase, phosphorylated Rb releases E2F1 and promotes the progression of cell cycle [35]. Loss-of-function alteration (D32fs) in *RB1* was found in HCC44 cells according to CCLE database (https://sites.broadinstitute.org/ccle), which might explain why AMG510 failed to arrest HCC44 cells at G1 phase. AMG510 persistently inhibited the phosphorylation of ERK up to 24 h in all tested cell lines except for H2122 cells, while inhibition on AKT phosphorylation was only observed in H358 cells and the level of phosphorylated AKT even increased in Calu-1 and HCC44 cells (Fig. 1d). Decreased phospho-Rb was found in H358 and Calu-1 cells but not HCC44 and H2122 cells (Fig. 1d), which is in accordance with the G1 phase arrest in H358 and Calu-1 cells. Thus, we found H358, Calu-1, MIA PaCa-2, SW837, and H23 cells were sensitive to AMG510, which might be associated with AMG510-induced G1 phase arrest.

$KRAS^{G12C}$-mutant cells developed acquired resistance after continuous exposure to AMG510

To monitor the occurrence of resistance to $KRas^{G12C}$ inhibitors in $KRAS^{G12C}$-mutant cells, we exposed sensitive H358, Calu-1, MIA PaCa-2, SW837, and H23 cells to increasing concentrations of AMG510 for about 3 months. Cells which developed acquired resistance to AMG510 were named as H358 R, Calu-1 R, MIA PaCa-2 R, SW837 R, or H23 R, respectively (Fig. 2a). Secondary mutation in the target is one of the most common causes leading to drug resistance. Sequencing of *KRAS* gene in five lines of resistant cells revealed that *KRAS* mutated back to wild-type in H358 R cells, while other resistant cells remained heterozygous $KRAS^{G12C}$ mutation (Fig. 2b). A recent study had reported that multiple mutations in *KRAS* at codons 13, 61, 68, 95, and 96 were detected in tumor tissues obtained from patients developed acquired resistance to MRTX849 [27]. However, no additional mutations at codons 13, 61, 68, 95, or 96 were detected in the newly established resistant cells (Fig. 2b and Supplementary Fig. 1a). As AMG510 has been approved by FDA for the treatment of $KRAS^{G12C}$-mutant NSCLC, we focused on $KRAS^{G12C}$-mutant NSCLC cells in following studies. We generated 2 lines of monoclonal cells from Calu-1 R cells, namely Calu-1 C and Calu-1 E. Calu-1 C/E cells displayed significant resistance to AMG510 (Fig. 2c) as well as two other $KRas^{G12C}$ inhibitors, ARS-1620 (Fig. 2d) and MRTX-849 (Fig. 2e). The resistance was sustained after withdrawing AMG510 for 33 days (Supplementary Fig. 1b). Similar to Calu-1 R cells, no additional mutation in *KRAS* was detected in Calu-1 C/E cells (Supplementary Fig. 1c). These results indicated that cells with acquired resistance to $KRas^{G12C}$ inhibitors were successfully established and Calu-1 C/E cells displayed durable and cross-resistance to $KRas^{G12C}$ inhibitors.

Activation of RTKs rendered $KRAS^{G12C}$-mutant cells resistant to AMG510

To explore the mechanisms of acquired resistance to AMG510 in Calu-1 C/E cells, we interrogated the PI3K and MPAK signaling pathways upon AMG510 treatment for 24 h in both resistant and parental cells. As shown in Fig. 3a, the basal level of phosphorylated ERK was dramatically elevated in Calu-1 C/E cells compared to that in parental cells. AMG510 inhibited the phosphorylation of ERK in Calu-1 cells but not in Calu-1 C/E cells. Similar results were observed in MIA PaCa-2 R and Calu-1 R cells (Supplementary Fig. 2a). Though the level of phosphorylated AKT decreased after treatment of AMG510 for 2 h in Calu-1 and H358 cells (Fig. 1b), we noticed that prolonged treatment of AMG510 resulted in rebound of phosphorylated AKT in most $KRas^{G12C}$-mutant cells (Fig. 1d, Fig. 3a and Supplementary Fig. 2a), which suggested that feedback activation of PI3K pathway in $KRAS^{G12C}$-mutant cells might be a common phenomenon. In addition, the level of phosphorylated Rb was less affected by AMG510 in resistant cells

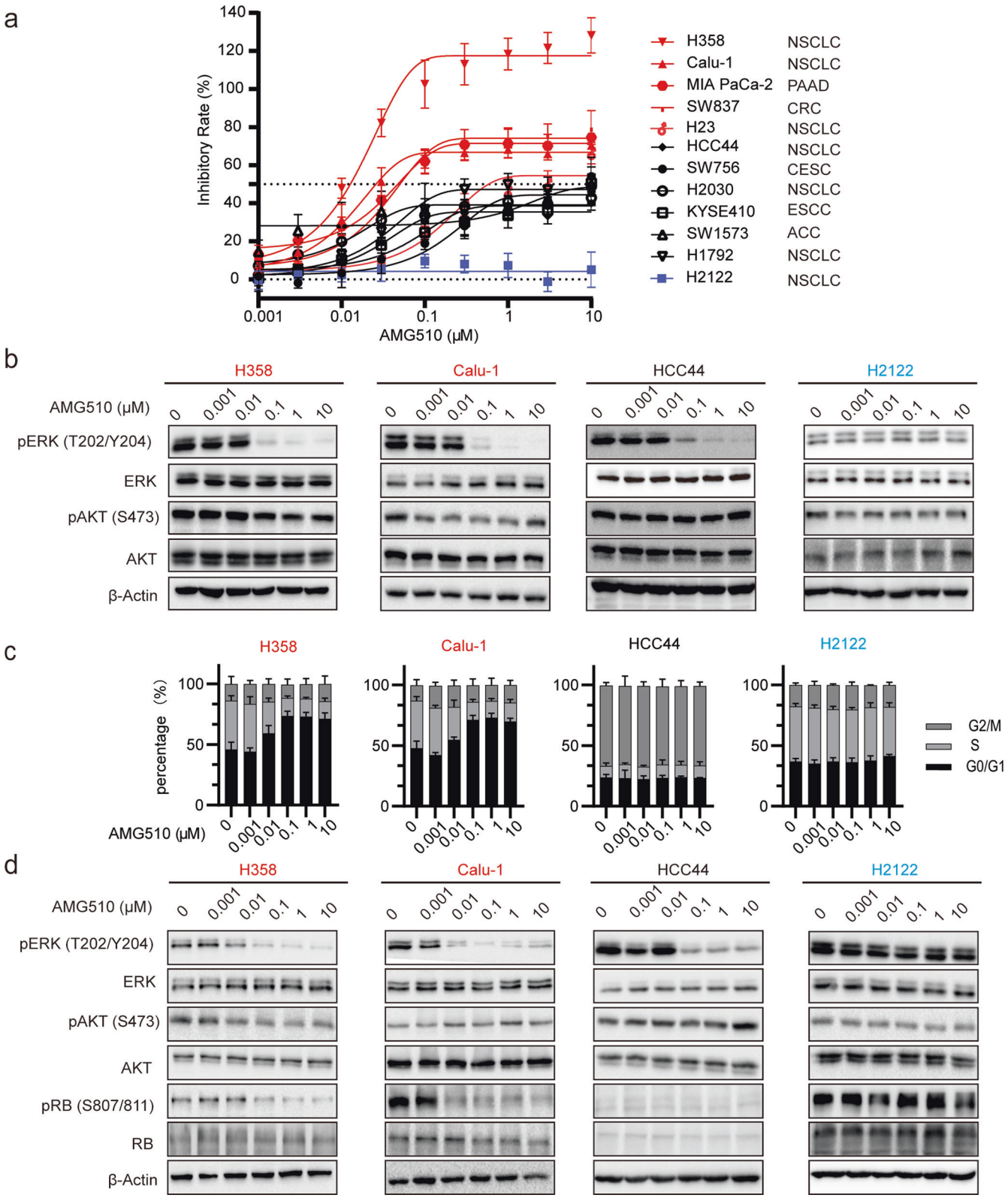

Fig. 1 AMG510 displayed variable anti-proliferative efficacy in *KRAS*^{G12C}-mutant cells. a *KRAS*^{G12C}-mutant cells derived from different tissue types were treated with gradient concentrations of AMG510 for 72 h and cell proliferation was measured by SRB assay ($n = 3$). NSCLC: Non-small cell lung cancer; PAAD: pancreatic adenocarcinoma; CRC: colorectal cancer; CSCC: cervical squamous cell carcinoma; ESCC: esophageal squamous cell carcinoma; ACC: adrenocortical carcinoma. **b** H358, Calu-1, HCC44 and H2122 cells were treated with indicated concentrations of AMG510 for 2 h. Cell lysates were subjected to Western blotting with the indicated antibodies. **c** H358, Calu-1, HCC44 and H2122 cells were incubated with indicated concentrations of AMG510 for 24 h and cell cycle distribution was analyzed with a flow cytometry ($n = 3$). **d** H358, Calu-1, HCC44, and H2122 cells were treated with indicated concentrations of AMG510 for 24 h. Cell lysates were then subjected to Western blotting with the indicated antibodies. Data were presented as mean ± SD or representative from at least three experiments.

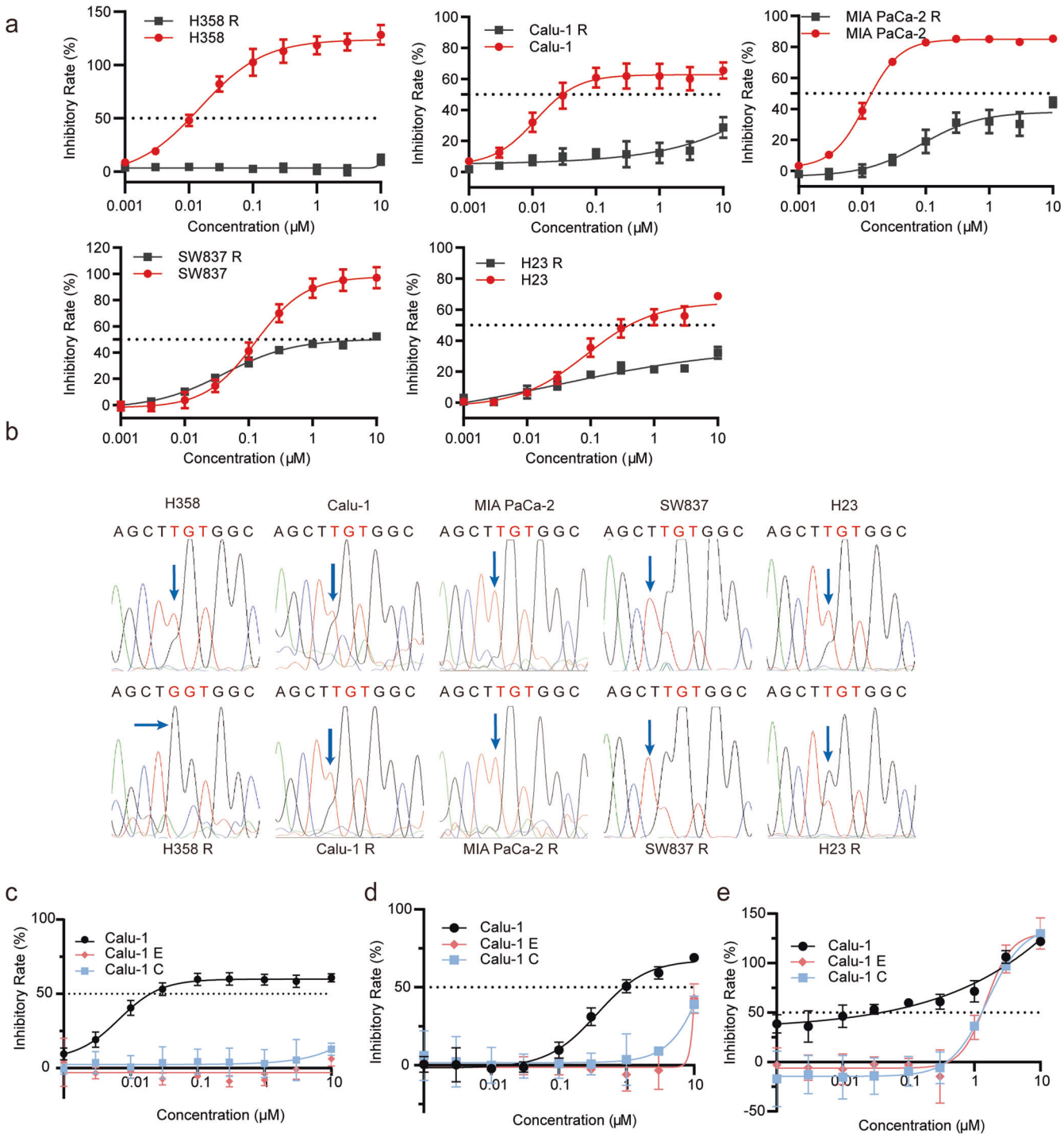

Fig. 2 ***Kras*^{G12C}-mutant cells developed acquired resistance after continuous exposure to AMG510. a** Parental and resistant cells were incubated with AMG510 for 72 h and cell proliferation was measured by SRB assay ($n = 3$). **b** Sanger sequencing of nucleotides of codon 12 and 13 of *KRAS*. **c-e** Calu-1 and Calu-1 C/E cells were incubated with AMG510 (**c**), ARS-1620 (**d**), or MRTX-849 (**e**) for 72 h and cell proliferation was measured by SRB assay ($n = 3$). Data were presented as mean ± SD from at least three experiments.

than that in parental cells. Consistently, AMG510 significantly arrested cells at G1 phase in parental cells, while it displayed marginal effect on cell cycle distribution in resistant cells (Fig. 3b and Supplementary Fig. 2b). In particular, AMG510 failed to act on the phosphorylation of AKT and ERK in H358 R cells which harbored wild type *KRAS* (Supplementary Fig. 2c).

KRas acts as a downstream effector of RTK signaling and activates MAPK and PI3K pathways [9, 32]. As we found higher level of phospho-ERK in Calu-1 C/E cells than that in parental cells (Fig. 3a), we applied phospho-RTK array to detect the level of phosphorylated RTKs in cells representing sensitive (Calu-1), intrinsic resistant (H2122), pooled acquired resistant (Calu-1 R) as well as monoclonal acquired resistant (Calu-1 C) cells. Higher level of phosphorylation of EGFR and Insulin Receptor (IR) was detected in Calu-1 R and Calu-1 C cells, and increased phospho-Insulin-like growth factor 1 receptor (IGF1R) was also detected in Calu-1 C cells (Fig. 3c, d). In addition, the level of phospho-EGFR or phospho-IGF1R was dramatically higher in intrinsic resistant

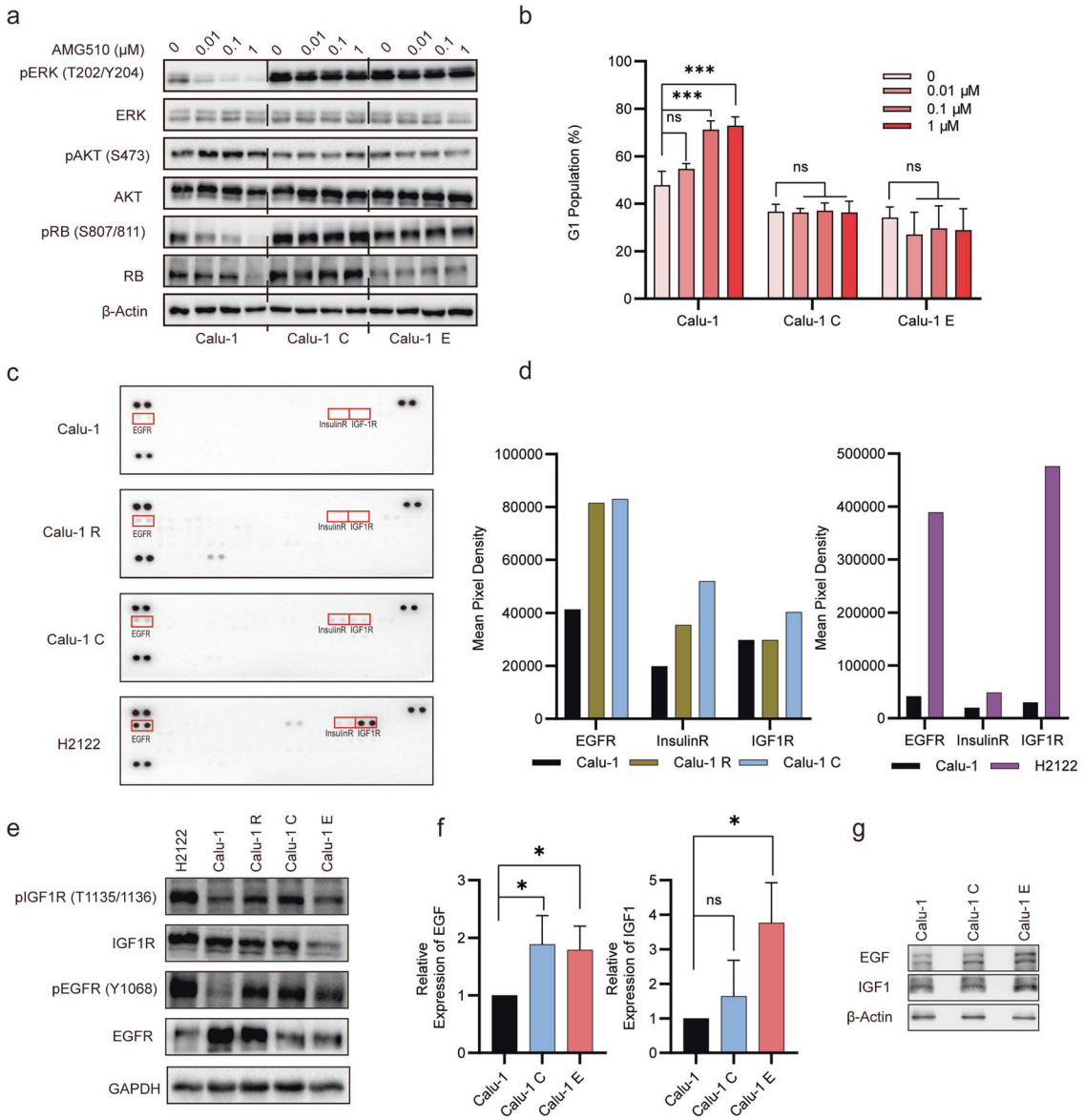

Fig. 3 Activation of RTKs rendered *KRAS*^{G12C}-mutant cells resistant to AMG510. **a** Calu-1 and Calu-1 C/E cells were treated with indicated concentrations of AMG510 for 24 h. Cell lysates were subjected to Western blotting with the indicated antibodies. **b** Calu-1 and Calu-1 C/E cells were incubated with AMG510 for 24 h and cell cycle distribution was analyzed with a flow cytometry ($n = 3$). Data were presented as mean ± SD. Differences between groups of vehicle control and AMG510 treatment were analyzed using one-way ANOVA with Tukey multiple group comparison test. ***$P < 0.001$; ns no significance. **c** Phospho-RTK array of Calu-1, Calu-1 R, Calu-1 C, and H2122 cells. Phosphorylated RTKs with difference between parental Calu-1 and resistant cells were highlighted with boxes. **d** Quantification of the Phospho-RTK array shown in **c** was measured by ImageJ. **e** Cell lysates from Calu-1, Calu-1 R, Calu-1 C/E, and H2122 cells were subjected to Western blotting with the indicated antibodies. **f** mRNA level of *EGF* and *IGF1* was measured by quantitative PCR in Calu-1 and Calu-1 C/E cells ($n = 3$). Data were presented as mean ± SD. Differences between indicated groups were analyzed using unpaired Student's *t*-test. *$P < 0.05$; ns no significance. **g** Protein levels of EGF and IGF1 were measured by Western blotting in Calu-1 and Calu-1 C/E cells.

H2122 cells than those in sensitive Calu-1 cells (Fig. 3c, d). Western blotting further confirmed that resistant Calu-1 C/E and H2122 cells displayed higher phosphorylation of EGFR and IGF1R than Calu-1 cells (Fig. 3e). We also observed elevated phospho-EGFR or phospho-IGF1R in MIA PaCa-2 R cells or SW837 R cells respectively, suggesting that differential RTKs were activated in different AMG510-resistant *KRAS*^{G12C}-mutant cells (Supplementary Fig. 2d). As total EGFR or IGF1R failed to increase in Calu-1 C/E cells compared to those in Calu-1 cells (Fig. 3e), EGFR and IGF1R might be activated by their ligands. Indeed, the expression of *EGF* and *IGF1* at mRNA level and protein level was enhanced in Calu-1 C/E cells compared to those in Calu-1 cells (Fig. 3f, g). IRS, Gab1, GRB2, SOS1 are common downstream adapters of RTKs, which remained largely unchanged in resistant cells (Supplementary Fig. 2e). Though, Axl was recently reported to play a critical role in mediating resistance to KRas^{G12C} inhibitors in Calu-1 cells [10], phosphorylated Axl slightly decreased in Calu-1 C/E cells compared to that in parental cells (Supplementary Fig. 2f). These results demonstrated that EGFR and/or IGF1R were activated in AMG510-resistant cells in a cell line-dependent manner, which might be due to elevated expression of EGF/IGF1.

Blockade of RTK signaling potentiated the activity of AMG510 in resistant cells

To explore whether overexpression of *EGF/IGF1* would mediate resistance to AMG510 in *KRAS*^{G12C}-mutant cells, we investigated

the impact of EGF or IGF1 on the efficacy of AMG510. As elevated phosphor-EGFR was observed in Calu-1 R and MIA PaCa-2 R cells, these cells were treated with AMG510 in the presence of EGF. As shown in Fig. 4a, EGF stimulation attenuated the activity of AMG510 in Calu-1 and MIA PaCa-2 cells. Similarly, Calu-1 and SW837 cells were treated with AMG510 in the presence of IGF1. IGF1 alleviated the activity of AMG510 in SW837 cells but not in Calu-1 cells (Fig. 4a), likely due to the relatively low expression of IGF1R in Calu-1 cells (Supplementary Fig. 3a). Consistently, EGF triggered acute increase in the phosphorylation of EGFR and downstream effector ERK as well as mild upregulation of phospho-AKT in Calu-1 and MIA PaCa-2 cells, which circumvented the effect of AMG510 on the phosphorylation of ERK and AKT (Fig. 4b). IGF1 stimulated the phosphorylation of AKT but not ERK in both Calu-1 and SW837 cells, which was in agreement with the knowledge that IGF1R signaling was mainly mediated by PI3K. AMG510 displayed less suppression on phospho-AKT in the presence of IGF (Fig. 4b). As we found that EGF and IGF1 activated PI3K/MAPK pathway in *KRAS*^{G12C}-mutant cells and conferred resistance to AMG510, we then tested whether inhibiting EGFR by erlotinib or IGF1R/InsulinR by linsitinib would overcome the resistance to AMG510. Erlotinib or linsitinib alone reduced phosphorylated EGFR or IGF1R, respectively in five lines of *KRAS*^{G12C}-mutant cells with acquired (Calu-1C, Calu-1 E, MIA PaCa-2 R, and SW837 R) or intrinsic (H2122 cells) resistance to AMG510. Combination of AMG510 with erlotinib or linsitinib potentiated the inhibition on phosphorylation of ERK and AKT, while triple combination further enhanced the inhibition (Fig. 4c). Accordingly, triple combination significantly elevated the activity against the colony formation in tested cell lines (Fig. 4d and Supplementary Fig. 3b). Collectively, EGFR and/or IGF1R mediated resistance to AMG510 dependent on the cellular contexts and inhibiting RTKs signaling could overcome the resistance.

Combination of the PI3Kα inhibitors with AMG510 synergistically inhibited proliferation of *KRAS*^{G12C}-mutant cells

Although the triple combination of inhibitors targeting EGFR, IGF1R, and Kras showed profound activity against resistant *KRAS*^{G12C}-mutant cells, this combination might lead to intolerable toxicity in clinical applications [36]. PI3K integrates signaling from RTKs and was found hyper-activated in AMG510-resisant Calu-1 C/E, H2122, and MIA PaCa-2 R cells after AMG510 treatment (Fig. 4c). We profiled the level of phosphorylated AKT and ERK in *KRAS*^{G12C}-mutant cell lines and found that phosphorylated AKT rather than phosphorylated ERK was negatively correlated with the anti-proliferative activity of AMG510 in *KRAS*^{G12C}-mutant cell lines (Fig. 5a). According to the cBioPortal database (www.cbioportal.org), mutation of *KRAS* and *PIK3CA* frequently co-existed in lung cancer, colorectal cancer and pancreatic cancer (Supplementary Fig. 4a). Therefore, targeting PI3K might improve the efficacy of AMG510 and overcome the resistance.

A novel PI3Kα-specific inhibitor CYH33 [37] was employed to combine with AMG510 in the resistant cells. Co-treatment of AMG510 and CYH33 synergistically inhibited the proliferation of Calu-1 R, MIA PaCa-2 R, SW837 R, and H23 R cells (Fig. 5b, c). The synergy was also observed in parental Calu-1 and HCC44 cells (Supplementary Fig. 4b). As AMG510 failed to inhibit proliferation of Calu-1 C and H2122 cells at the concentration below 10 μM, we evaluated the combinatorial effect with the Bliss independence model [31] at the concentration of 10 μM. As shown in Fig. 5c and Supplementary Fig. 4b, CYH33 combined with AMG510 showed slight synergism in Calu-1 C and H2122 cells at the concentration of 10 μM. To further elucidate the underlying mechanism of the synergism, we interrogated the KRas signaling. Though adaptive activation of AKT was detected after Calu-1 or HCC44 cells were incubated with AMG510 for 24 h (Fig. 1d), the combination of AMG510 with CYH33 showed persistent suppression on phospho-AKT, phospho-ERK and phospho-S6 in sensitive Calu-1 and resistant HCC44 cells. However, this combination had little activity on the phosphorylation of ERK in Calu-1 C cells, which may explain the mild inhibition on the proliferation of Calu-1 C cells (Fig. 5d). In summary, the combination of the CYH33 and AMG510 displayed synergistic effect in most *KRAS*^{G12C}-mutant cell lines and overcame both intrinsic and acquired resistance to AMG510.

Combination of the CYH33 with AMG510 synergistically inhibited the growth of xenografts derived from *KRAS*^{G12C}-mutant cells

The combination of AMG510 and CYH33 was further investigated in mice bearing xenografts derived Calu-1 C cells. As shown in Fig. 6a and Supplementary Fig. 5a, monotherapy of AMG510 or CYH33 slightly inhibited the growth of Calu-1 C xenografts, yielding T/C values of 65.8% or 71.2%. Co-administration of AMG510 and CYH33 significantly elevated the efficacy of monotherapy (T/C value of 34.0%). No significant loss of body weight was detected in mice during the treatment (Supplementary Fig. 5b), indicating well tolerance to the combination therapy. Accordingly, AMG510 reduced the phosphorylation of ERK but not AKT, while CYH33 inhibited the phosphorylation of AKT rather than ERK. Combination of AMG510 and CYH33 displayed enhanced activity to attenuate the phosphorylation of AKT, ERK, and S6 (Fig. 6b).

We also examined the efficacy of combined treatment with CYH33 and AMG510 in mice bearing xenografts derived from parental Calu-1 cells. AMG510 significantly inhibited the growth of Calu-1 xenografts with a T/C value of 12.3%, while CYH33 alone failed to inhibit the tumor growth (Fig. 6c). Combination of CYH33 and AMG510 further enhanced the inhibition on tumor growth with a T/C value of 2.6% and complete regression was observed in two out of six mice (Fig. 6c and Supplementary Fig. 5c). Accordingly, the combination simultaneously blocked phosphorylation of AKT and ERK, resulted in enhanced inhibition on phosphorylation of S6 (Fig. 6d), which might lead to a sustained tumor regression. The treatment was withdrawn after administration for 21 days. Xenografts relapsed rapidly in mice previously treated with AMG510, while the tumors remained quiescent in mice previously treated concurrently with CYH33 and AMG510 (Fig. 6c). To determine the effect of combined CYH33 and AMG510 on the relapsed tumors upon AMG510 treatment, mice previously treated with AMG510 were grouped to receive AMG510 alone or the combination of AMG510 and CYH33. As shown in Fig. 6e and Supplementary Fig. 5d, co-administration of AMG510 and CYH33 showed greater inhibition on tumor growth than AMG510 alone. Thus, combined CYH33 and AMG510 treatment exhibited prolonged inhibition on tumor growth and overcame acquired resistance to AMG510 in Calu-1 C xenografts.

DISCUSSION

The emerging of KRas^{G12C} inhibitors heralds a new era in precision medicine for cancer patients harboring *KRAS*^{G12C} mutation. However, acquired resistance has been observed in preclinical and clinical settings. In this study, we generated a series of cell lines with acquired resistance to AMG510 and found that differential activation of RTKs rendered resistance to AMG510 in different cellular contexts by maintaining the activation of MAPK/PI3K pathway. Simultaneous inhibition of EGFR and IGF1R restored sensitivity to AMG510 in resistant cells. However, triple combination of these inhibitors might be intolerable in clinical settings. We found phosphorylated AKT negatively correlated with the anti-proliferative activity of AMG510 in *KRAS*^{G12C}-mutant cell lines and concurrently targeting PI3Kα and KRas^{G12C} exhibited synergistic effect against parental and resistant *KRAS*^{G12C}-mutant cells in vitro and in vivo. These findings revealed the potential mechanism rendering acquired resistance to KRas^{G12C} inhibitors and provided a mechanistic rationale combining PI3Kα inhibitors with KRas^{G12C} inhibitors to treat *KRAS*^{G12C}-mutant cancers.

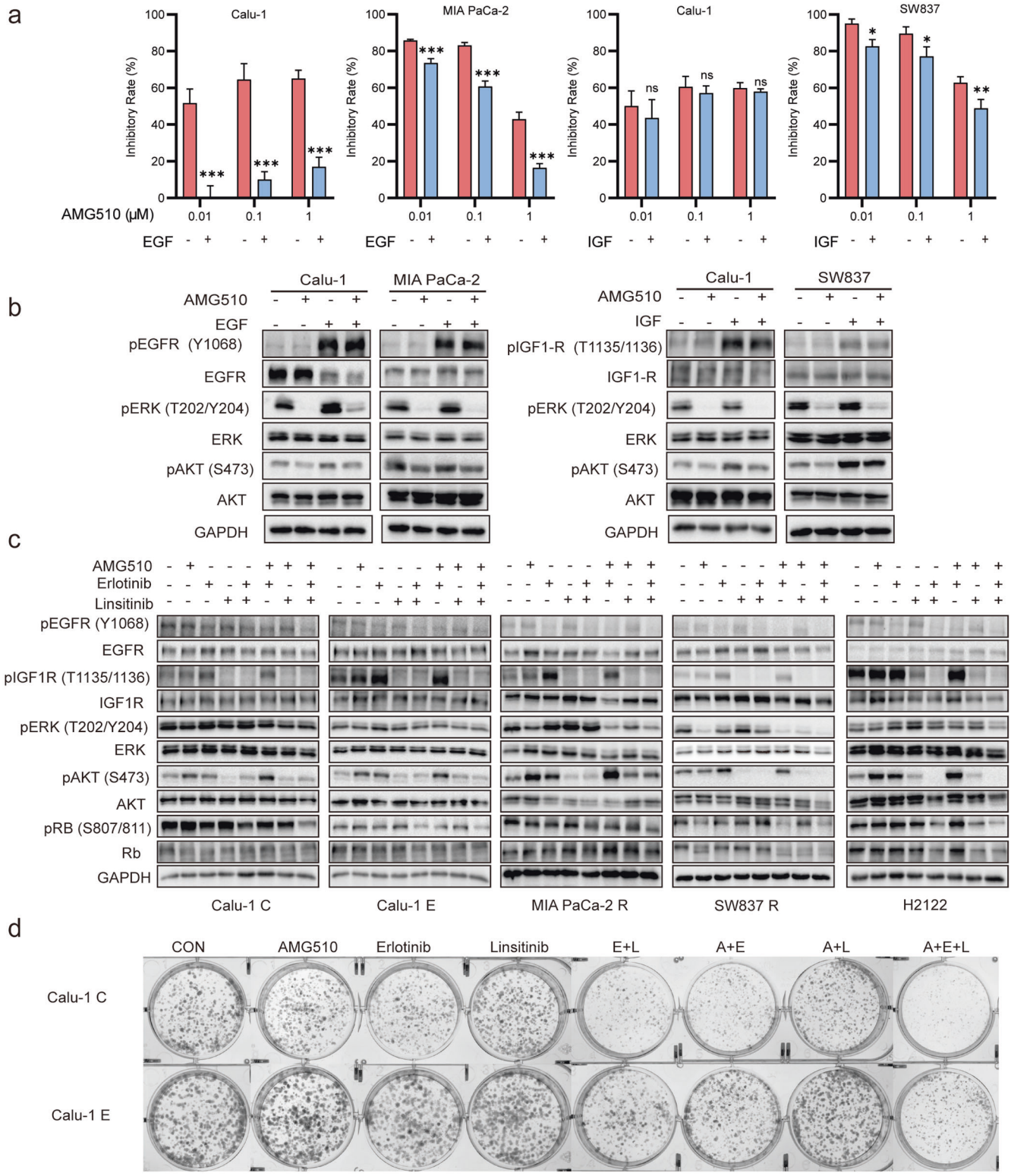

Fig. 4 Blockade of RTKs signaling potentiated the activity of AMG510 in resistant cells. a Calu-1, MIA PaCa-2, and SW837 cells were treated with AMG510 in the presence of EGF/IGF (50 ng/mL) or not for 72 h and cell proliferation was measured by SRB assay ($n = 3$). Data were presented as mean ± SD. Differences between indicated groups were analyzed using unpaired Student's *t*-test. $^{*}P < 0.05$; $^{**}P < 0.01$; $^{***}P < 0.001$; ns no significance. **b** Calu-1, MIA PaCa-2, and SW837 cells were incubated with EGF or IGF (50 ng/mL) for 15 min, then concurrently treated with 1 μM of AMG510 for 2 h. Cell lysates were subjected to Western blotting with the indicated antibodies. **c** Calu-1 C/E, H2122, MIA PaCa-2 R, and SW837 R cells were treated with AMG510 (10 μM), linsitinib (1 μM) or erlotinib (10 μM) alone or in combination as indicated for 24 h, and cell lysates were then subjected to Western blotting with the indicated antibodies. **d** Colony formation assay of Calu-1 C/E cells incubated with AMG510 (10 μM), linsitinib (1 μM), erlotinib (10 μM) alone or the indicated combinations for 10 days.

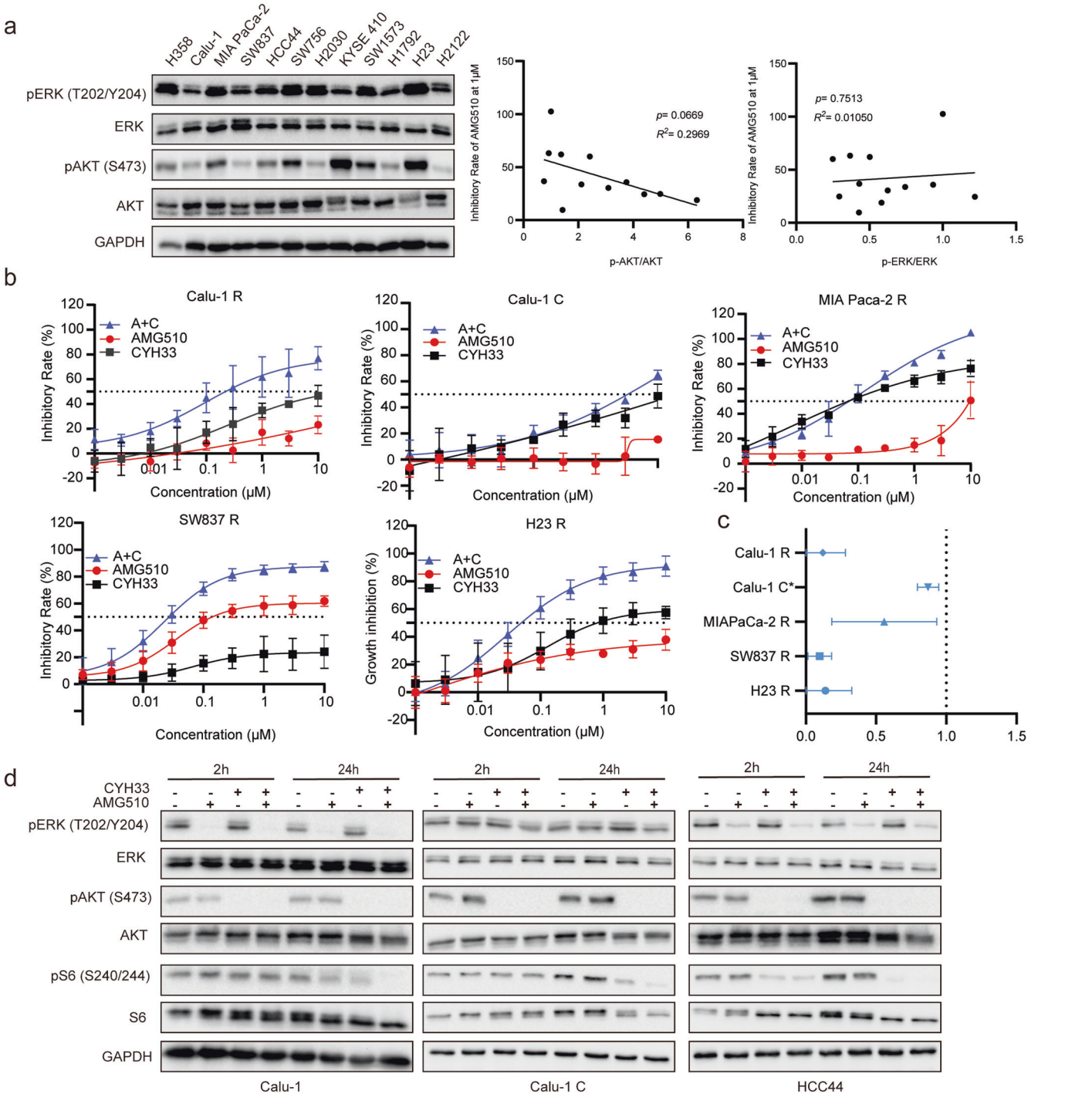

Fig. 5 Combination of the PI3Kα inhibitor with AMG510 synergistically inhibited proliferation of *KRAS*^{G12C}-mutant cells. a Cell lysates of *KRAS*^{G12C}-mutated cells were subjected to Western blotting with the indicated antibodies. The intensity of protein bands was quantified by Image J. Pearson correlation of the level of p-AKT/AKT or p-ERK/ERK and inhibitory rate of proliferation by AMG510 at 1 μM was performed. Calu-1 R, Calu-1 C, MIA PaCa-2 R, SW837 R, and H23 R cells were incubated with AMG510 and CYH33 alone or concurrently for 72 h and cell proliferation was measured by SRB assay ($n = 3$) (**b**). The CI values of the combination of AMG510 and CYH33 were determined by CalcuSyn software in Calu-1 R, MIA PaCa-2 R, H23 R, and SW837 R cells or by the Bliss independence model in Calu-1 C cells ($n = 3$) (**c**). Data were presented as mean ± SD. **d** Calu-1, Calu-1 C, and HCC44 cells were treated with AMG510 or CYH33 alone or concurrently for 2 or 24 h. Cell lysates were subjected to Western blotting with the indicated antibodies. (1 μM of AMG510 and 1 μM of CYH33 for Calu-1 and HCC44 cells; 10 μM of AMG510 and 10 μM of CYH33 for Calu-1 C cells).

RTKs are common upstream receptors of KRas, which transduce extracellular signals to the intracellular pathways. We found that activation of RTKs conferred *KRAS*^{G12C}-mutant cells to develop resistance to AMG510. It has been recently reported that EGFR was hyperactive in *KRAS*^{G12C}-mutant CRC cell lines compared to that in NSCLC cell lines, which might contribute to the intrinsic resistance of CRC to KRas^{G12C} inhibitors [24]. We found that differential RTKs were activated in different AMG510-resistant cells. For example,

MIA PaCa-2 R and Calu-1 R cells depended largely on EGFR-ERK axis, SW837 R cells relied more on IGF1R-AKT axis, while H23 R cells might acquire activation of other RTKs. Similarly, treatment of a couple lines of *KRAS*^{G12C}-mutant NSCLC cells with the KRas^{G12C} inhibitor ARS-1620 for 48 h resulted in adaptive activation of RTKs [23]. These results suggested that development of acquired resistance might be dependent on differential RTKs in distinct *KRAS*^{G12C}-mutant cancer cells. IGF1R was found to maintain the activation of PI3K pathway to induce epithelial-mesenchymal transition and resistance to KRas^{G12C} inhibitors [38], while *MET* amplification conferred resistance to AMG510 in H23 cells [39]. Upregulation of ligands is one of the crucial mechanisms to activate RTKs. We detected increased expression level of growth factors such as EGF and IGF1 in resistant Calu-1 cells, which was consistent with the activation of EGFR and IR/IGF1R. In agreement with our observation, the expression of *EGF* was reported to rebound after treatment with ARS1620 for 48–72 h in *KRAS*^{G12C}-mutatant NSCLC cells [26]. However, the mechanism of induction

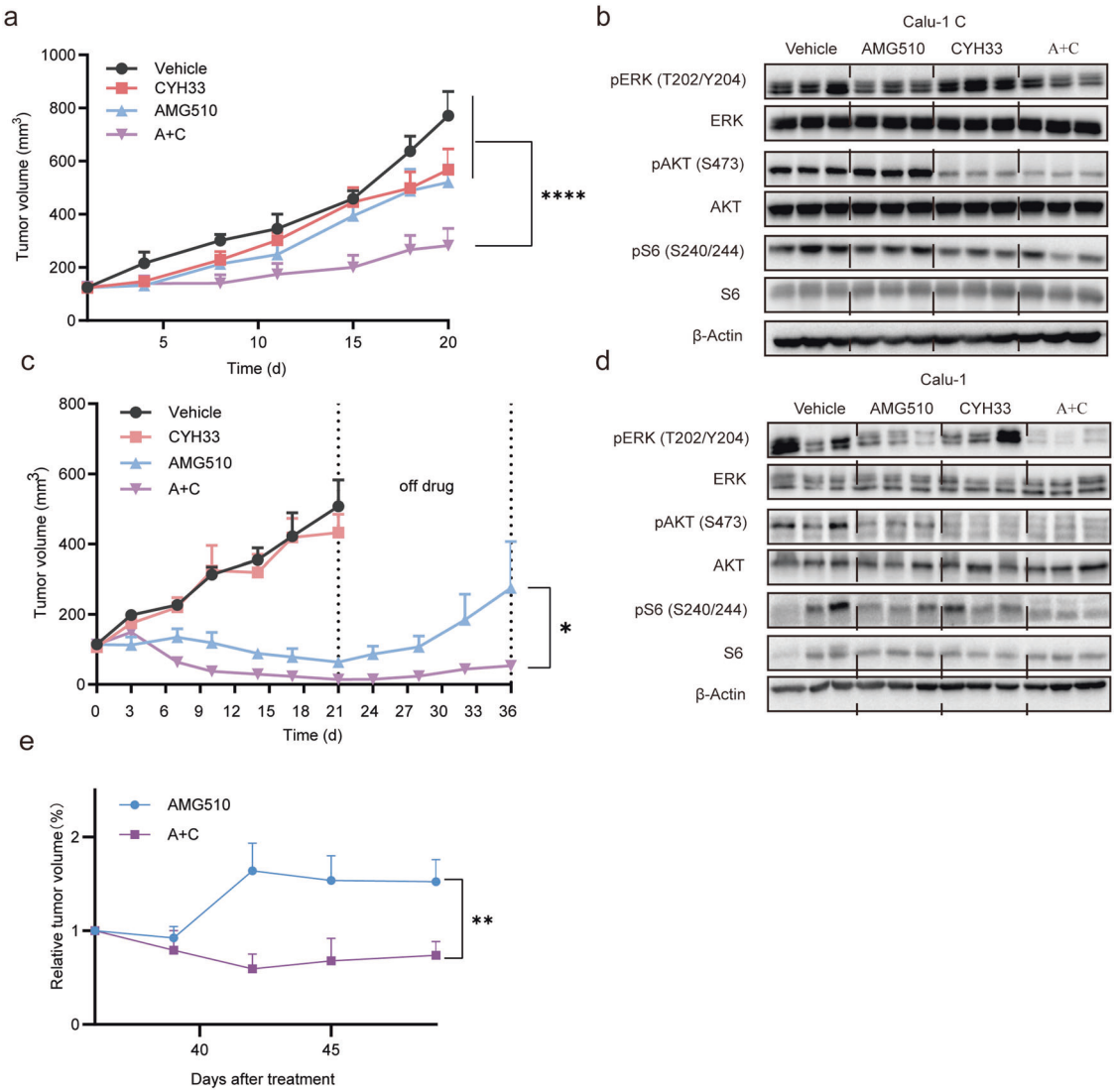

Fig. 6 Combination of CYH33 with AMG510 synergistically inhibited the growth of xenografts derived from *KRAS*^{G12C}-mutant cells. **a** Randomly grouped nude mice bearing Calu-1 C xenografts were administered orally with a vehicle control, AMG510 (30 mg/kg), CYH33 (20 mg/kg), or a combination of AMG510 and CYH33 once a day for 20 days ($n = 6$). Tumor volume was measured twice a week. Data were presented as mean ± SEM. Differences between the indicated groups were analyzed using Two-way ANOVA with Tukey multiple group comparison test. ****$P < 0.0001$. **b** Randomly grouped nude mice bearing Calu-1 C xenografts were administered orally with a vehicle control, AMG510 (30 mg/kg), CYH33 (20 mg/kg), or a combination of AMG510 and CYH33 for 24 h. On the next day, the mice were dosed 2 h before sacrifice and tumors were collected and subjected to Western blotting with the indicated antibodies. **c** Randomly grouped nude mice bearing Calu-1 xenografts were administered orally with a vehicle control, AMG510 (30 mg/kg), CYH33 (20 mg/kg), or a combination of AMG510 and CYH33 once a day for 21 days ($n = 6$). At the end of 21 days, the nude mice treated with AMG510 alone or the combination of AMG510 and CYH33 were off treatment for another 14 days. Tumor volume was measured twice a week ($n = 6$). Data were presented as mean ± SEM. Differences between the indicated groups were analyzed using Two-way ANOVA with Tukey multiple group comparison test. *$P < 0.05$. **d** Randomly grouped nude mice bearing Calu-1 xenografts were administered orally with a vehicle control, AMG510 (30 mg/kg), CYH33 (20 mg/kg), or a combination of AMG510 and CYH33 for 24 h. On the next day, the mice were dosed 2 h before sacrifice. Tumors were collected and subjected to Western blotting with the indicated antibodies. **e** Mice form AMG510-treated group in **c** were divided into two groups and treated with AMG510 alone or concurrently with CYH33. Tumor volume was measured twice a week ($n = 3$). Differences between the indicated groups were analyzed using Two-way ANOVA with Tukey multiple-group comparison test. **$P < 0.01$. Data were presented as mean ± SEM.

of growth factors in resistant cells remains unknown and deserves further investigation. Simultaneously inhibiting EGFR and IGF1R restored the sensitivity of resistant cells to AMG510, which was associated with blockade of PI3K and MPAK signaling as well as Rb phosphorylation, further supporting that activation of RTKs mediated resistance to $KRas^{G12C}$ inhibitors. Though several studies also reported that RTK inhibitors potentiated the efficacy of $KRas^{G12C}$ inhibitors [23, 40, 41], differential RTKs are required to be blocked as distinct RTKs might mediate the resistance dependent on cellular contexts.

PI3K integrates signaling from various RTKs and plays an important role as a downstream effector in Ras signaling [9, 33, 40, 42]. We revealed that activation of PI3K might be critical to development resistance to $KRAS^{G12C}$ inhibitors. Long-term treatment with AMG510 induced rebound of phospho-AKT, which has been commonly observed in $KRAS^{G12C}$-mutant cells [10, 25]. Hyper-phosphorylation of AKT was also found in most cells with acquired resistance to AMG510 established in this study. Accordingly, concurrently targeting PI3Kα and $KRas^{G12C}$ displayed synergistic activity against parental and resistant $KRAS^{G12C}$-mutant cells in vitro and in vivo, which is also supported by a recent drug combination screening [25]. Our results also suggested that the combination of AMG510 and CYH33 might prevent tumor recurrence. Of note, the PI3Kα inhibitor CYH33 improved the anti-tumor activity of AMG510 and overcame the resistance at a lower dosage than GDC0941 [10, 38]. Although the combination of PI3K and MAPK inhibitors was intolerable and led to dose-limiting toxicities in vivo [43], AMG510 combined with CYH33 had little effect on the body weight of mice, suggesting the favorable safety profile. Co-existence of *PIK3CA* and *KRAS* mutation is often found in NSCLC, CRC, and PDAC patients according to the cBioPortal database. The combination deserves further investigation in preclinical and clinical studies.

In conclusion, we found that $KRAS^{G12C}$-mutant cells depended on preferential RTKs during the development of acquired resistance to AMG510. Concurrently targeting PI3Kα and $KRas^{G12C}$ delayed and overcame the resistance to $KRas^{G12C}$ inhibitors. These findings provide a mechanistic rationale to test $KRas^{G12C}$ inhibitors in combination with PI3Kα inhibitors for treating $KRAS^{G12C}$-mutant cancers in future clinical trials.

ACKNOWLEDGEMENTS

This work was supported by National Natural Science Foundation of China (82104199, 82173832 and 81973345), the Lingang Laboratory (LG202103-02-03) and Science and Technology Commission of Shanghai Municipality (22ZR1474400).

AUTHOR CONTRIBUTIONS

LHM, YXW, and WLQ conceived the study and wrote the manuscript. WLQ carried most of the experiments. HYL, JTD, and XZ performed part of the cell proliferation and Western blotting assay. YW established AMG510-acquired resistance cell lines. LX conducted part of animal experiments. LHM and YXW supervised the study. All authors proofread the manuscript and approved to submit the final manuscript.

ADDITIONAL INFORMATION

Supplementary information The online version contains supplementary material available at https://doi.org/10.1038/s41401-022-01015-0.

Competing interests: The authors declare no competing interests.

REFERENCES

1. Hofmann MH, Gerlach D, Misale S, Petronczki M, Kraut N. Expanding the reach of precision oncology by drugging All KRAS mutants. Cancer Discov. 2022;12:924–37.
2. Khan I, Rhett JM, O'Bryan JP. Therapeutic targeting of RAS: New hope for drugging the "undruggable". Biochim Biophys Acta Mol Cell Res. 2020;1867:118570.
3. Schaber MD, Garsky VM, Boylan D, Hill WS, Scolnick EM, Marshall MS, et al. Ras interaction with the gtpase-activating protein (Gap). Proteins. 1989;6:306–15.
4. Lu S, Jang H, Gu S, Zhang J, Nussinov R. Drugging Ras GTPase: a comprehensive mechanistic and signaling structural view. Chem Soc Rev. 2016;45:4929–52.
5. Banno K, Yanokura M, Iida M, Masuda K, Aoki D. Carcinogenic mechanisms of endometrial cancer: involvement of genetics and epigenetics. J Obstet Gynaecol Res. 2014;40:1957–67.
6. Siqi Li ABCMC. A model for RAS mutation patterns in cancers: finding the sweet spot. Nat Rev Cancer. 2018;18:767–77.
7. Balmain A, Pragnell IB. Mouse skin carcinomas induced in vivo by chemical carcinogens have a transforming Harvey-ras oncogene. Nature. 1983;303:72–4.
8. Sukumar S, Notario V, Martin-Zanca D, Barbacid M. Induction of mammary carcinomas in rats by nitrosomethyl-urea involves the malignant activation of the H-ras-1 locus by single point mutations. Nature. 1983;306:658–61.
9. Cox AD, Fesik SW, Kimmelman AC, Luo J, Der CJ. Drugging the undruggable RAS: mission possible? Nat Rev Drug Discov. 2014;13:828–51.
10. Canon J, Rex K, Saiki AY, Mohr C, Cooke K, Bagal D, et al. The clinical KRAS(G12C) inhibitor AMG 510 drives anti-tumour immunity. Nature. 2019;575:217–23.
11. Janes MR, Zhang J, Li LS, Hansen R, Peters U, Guo X, et al. Targeting KRAS mutant cancers with a covalent G12C-Specific inhibitor. Cell. 2018;172:578–89.e17.
12. Johnson ML, Ou SHI, Barve M, Rybkin II, Papadopoulos KP, Leal TA, et al. Activity and safety of Adagrasib (MRTX849) in patients with colorectal cancer (CRC) and other solid tumors harboring a KRAS G12C mutation. Eur J Cancer. 2020;138:S2.
13. Jänne PA, Rybkin II, Spira AI, Riely GJ, Papadopoulos KP, Sabari JK, et al. Activity and safety of Adagrasib (MRTX849) in advanced/ metastatic non–small-cell lung cancer (NSCLC) harboring KRAS G12C mutation. Eur J Cancer. 2020;138:S1–2.
14. Patricelli MP, Janes MR, Li L-S, Hansen R, Peters U, Kessler LV, et al. Selective inhibition of oncogenic KRAS output with small molecules targeting the inactive state. Cancer Discov. 2016;6:316–29.
15. Lito P, Solomon M, Li LS, Hansen R, Rosen N. Allele-specific inhibitors inactivate mutant KRAS G12C by a trapping mechanism. Science. 2016;351:604–8.
16. Li H-y, Qi W-l, Wang Y-x, Meng L-h. Covalent inhibitor targets KRasG12C: a new paradigm for drugging the undruggable and challenges ahead. Genes Dis. 2021; https://doi.org/10.1016/j.gendis.2021.08.011.
17. Lanman BA, Allen JR, Allen JG, Amegadzie AK, Ashton KS, Booker SK, et al. Discovery of a covalent inhibitor of KRAS(G12C) (AMG 510) for the treatment of solid tumors. J Med Chem. 2020;63:52–65.
18. Jiao D, Yang S. Overcoming resistance to drugs targeting KRAS mutation. Innovation. 2020;1:100035.
19. Nakajima EC, Drezner N, Li X, Mishra-Kalyani PS, Liu Y, Zhao H, et al. FDA Approval Summary: Sotorasib for KRAS G12C-mutated metastatic NSCLC. Clin Cancer Res. 2022;28:1482–6.
20. Ou SI, Janne PA, Leal TA, Rybkin, II, Sabari JK, Barve MA, et al. First-in-human phase I/IB dose-finding study of Adagrasib (MRTX849) in patients with advanced KRAS(G12C) solid tumors (KRYSTAL-1). J Clin Oncol. 2022;40:JCO2102752.
21. Soria JC, Ohe Y, Vansteenkiste J, Reungwetwattana T, Chewaskulyong B, Lee KH, et al. Osimertinib in untreated EGFR-mutated advanced non-small-cell lung cancer. N Engl J Med. 2018;378:113–25.
22. Peters S, Camidge DR, Shaw AT, Gadgeel S, Ahn JS, Kim DW, et al. Alectinib versus Crizotinib in Untreated ALK-positive non-small-cell lung cancer. N Engl J Med. 2017;377:829–38.
23. Ryan MB, Fece de la Cruz F, Phat S, Myers DT, Wong E, Shahzade HA, et al. Vertical pathway inhibition overcomes adaptive feedback resistance to KRAS(G12C) inhibition. Clin Cancer Res. 2020;26:1633–43.
24. Amodio V, Yaeger R, Arcella P, Cancelliere C, Lamba S, Lorenzato A, et al. EGFR blockade reverts resistance to KRAS(G12C) inhibition in colorectal cancer. Cancer Discov. 2020;10:1129–39.
25. Misale S, Fatherree JP, Cortez E, Li CD, Bilton S, Timonina D, et al. KRAS G12C NSCLC models are sensitive to direct targeting of KRAS in combination with PI3K inhibition. Clin Cancer Res. 2019;25:796–807.
26. Xue JY, Zhao Y, Aronowitz J, Mai TT, Vides A, Qeriqi B, et al. Rapid non-uniform adaptation to conformation-specific KRAS(G12C) inhibition. Nature. 2020;577:421–5.
27. Awad MM, Liu S, Rybkin II, Arbour KC, Dilly J, Zhu VW, et al. Acquired resistance to KRAS(G12C) inhibition in cancer. N Engl J Med. 2021;384:2382–93.
28. Liu XL, Wang BB, Wang Y, Wang YX, Yang CH, Tan C, et al. Unbiased screening reveals that blocking exportin 1 overcomes resistance to PI3Kalpha inhibition in breast cancer. Signal Transduct Target Ther. 2019;4:49.
29. Li X, Tong LJ, Ding J, Meng LH. Systematic combination screening reveals synergism between rapamycin and sunitinib against human lung cancer. Cancer Lett. 2014;342:159–66.
30. Shi JJ, Chen SM, Guo CL, Li YX, Ding J, Meng LH. The mTOR inhibitor AZD8055 overcomes tamoxifen resistance in breast cancer cells by down-regulating HSPB8. Acta Pharmacol Sin. 2018;39:1338–46.

31. Tang J, Wennerberg K, Aittokallio T. What is synergy? The Saariselka agreement revisited. Front Pharmacol. 2015;6:181.
32. Ni D, Li X, He X, Zhang H, Zhang J, Lu S. Drugging K-Ras(G12C) through covalent inhibitors: mission possible? Pharmacol Ther. 2019;202:1–17.
33. Liu P, Wang Y, Li X. Targeting the untargetable KRAS in cancer therapy. Acta Pharm Sin B. 2019;9:871–9.
34. Rodenhuis, S. ras and human tumors. Semin Cancer Biol. 1992;3:241–7.
35. Rubin SM, Sage J, Skotheim JM. Integrating old and new paradigms of G_1/S control. Mol Cell. 2020;80:183–92.
36. Molina-Arcas M, Moore C, Rana S, van Maldegem F, Mugarza E, Romero-Clavijo P, et al. Development of combination therapies to maximize the impact of KRAS-G12C inhibitors in lung cancer. Sci Transl Med. 2019;11:eaaw7999.
37. Xiang HY, Wang X, Chen YH, Zhang X, Tan C, Wang Y, et al. Identification of methyl (5-(6-((4-(methylsulfonyl)piperazin-1-yl)methyl)-4-morpholinopyrrolo[2,1-f][1,2,4]triazin-2-yl)-4-(trifluoromethyl)pyridin-2-yl)carbamate (CYH33) as an orally bioavailable, highly potent, PI3K alpha inhibitor for the treatment of advanced solid tumors. Eur J Med Chem. 2021;209:112913.
38. Adachi Y, Ito K, Hayashi Y, Kimura R, Tan TZ, Yamaguchi R, et al. Epithelial-to-mesenchymal transition is a cause of both intrinsic and acquired resistance to KRAS G12C inhibitor in KRAS G12C-mutant non-small cell lung cancer. Clin Cancer Res. 2020;26:5962–73.
39. Suzuki S, Yonesaka K, Teramura T, Takehara T, Kato R, Sakai H, et al. KRAS inhibitor resistance in MET-amplified KRAS (G12C) non-small cell lung cancer induced By RAS- and non-RAS-mediated cell signaling mechanisms. Clin Cancer Res. 2021;27:5697–707.
40. Ryan MB, Corcoran RB. Therapeutic strategies to target RAS-mutant cancers. Nature. 2018;15:709–20.
41. Hallin, J, Engstrom, LD, Hargis, L, Calinisan, A, Aranda, R, Briere, DM. The KRAS(G12C) inhibitor MRTX849 provides insight toward therapeutic susceptibility of KRAS-mutant cancers in mouse models and patients. Cancer Discov. 2020;10:54–71.
42. Moore AR, Rosenberg SC, McCormick F, Malek S. RAS-targeted therapies: is the undruggable drugged? Nat Rev Drug Discov. 2020;19:533–52.
43. Shimizu T, Tolcher AW, Papadopoulos KP, Beeram M, Rasco DW, Smith LS, et al. The clinical effect of the dual-targeting strategy involving PI3K/AKT/mTOR and RAS/MEK/ERK pathways in patients with advanced cancer. Clin Cancer Res. 2012;18:2316–25.